

Fission Matrix Interpolation For The Tfm Approach Based On A Local Correlated Sampling Technique For Fast Spectrum Heterogeneous Reactors

A. Laureau, L. Buiron, B. Fontaine, V. Pascal

▶ **To cite this version:**

A. Laureau, L. Buiron, B. Fontaine, V. Pascal. Fission Matrix Interpolation For The Tfm Approach Based On A Local Correlated Sampling Technique For Fast Spectrum Heterogeneous Reactors. M&C - 2017 International Meeting on Mathematics and Computation Supercomputing, Reactor Physics and Nuclear and Biological Applications, Apr 2017, Jeju, South Korea. cea-02434553

HAL Id: cea-02434553

https://cea.hal.science/cea-02434553

Submitted on 10 Jan 2020

HAL is a multi-disciplinary open access archive for the deposit and dissemination of scientific research documents, whether they are published or not. The documents may come from teaching and research institutions in France or abroad, or from public or private research centers.

L'archive ouverte pluridisciplinaire **HAL**, est destinée au dépôt et à la diffusion de documents scientifiques de niveau recherche, publiés ou non, émanant des établissements d'enseignement et de recherche français ou étrangers, des laboratoires publics ou privés.

M&C 2017 - International Conference on Mathematics & Computational Methods Applied to Nuclear Science & Engineering, Jeju, Korea, April 16-20, 2017, on USB (2017)

Fission Matrix Interpolation for the TFM Approach Based on a Local Correlated Sampling Technique for Fast Spectrum Heterogeneous Reactors

Axel Laureau, Laurent Buiron, Bruno Fontaine, Vincent Pascal

CEA, DEN, DER, Cadarache 13 108 Saint-Paul les Durance Cedex
axel.laureau@cea.fr

Abstract - *Reactor safety analysis requires complex coupled multiphysics calculations modeling the full core evolution during various accidental situations. Such calculation codes rely on physical models adapted to the physics of the simulated reactor concept. In this frame, the innovative Transient Fission Matrix (TFM) neutronic approach, based on a conversion of the Monte Carlo response in Green functions characterizing the local transport in the reactor and initialy developed for other kinds of reactors, has been successfully applied on one dimensional sodium fast reactors using the correlated sampling technique as detailed in this article. This method takes into account the sensitivity of the neutron transport to local perturbations in order to estimate on the fly the matrices variations due to a given perturbation distribution. This model provides an accurate estimation of the reactivity and of the power distribution in the core during the accident, including the influence of the sodium density distribution in the plenum. This article also illustrates the applications of this neutronic model on sodium fast reactors for small to large perturbations of the system, and point kinetic feedback coefficients evaluations.*

I. INTRODUCTION

To perform reliable reactor safety analysis, accidental transients such as Unprotected Transient Over Power (UTOP) or Loss Of Flow (ULOF) accidents have to be calculated with coupled multiphysics modelling codes at the full core scale. This requires optimized physical models for neutronic and thermalhydraulics at least. In this frame, the innovative Transient Fission Matrix (TFM) neutronic approach has been developed as an hybrid approach between stochastic and deterministic codes, to allow fast and precise calculations during transient simulations. This approach described in [1] condenses the spatial and temporal reactor response obtained by Monte Carlo calculations in fission and time matrices that are intended to be used to solve deterministicaly the kinetic equations of the prompt and delayed neutrons during the transient evolution. The reactor behavior is then estimated using a single Monte Carlo calculation prior to the transient evaluation, and finally the neutron kinetics uses directly these matrices without additional calculation. This TFM approach provides a precise estimation of the neutron flux redistribution and of the reactivity during the transient with a reduced computation time.

One of the main challenges is to model the matrix variations during the transient: due to thermal feedbacks the neutron transport is modified. To take this into account without recalculating the matrices at each time step of the transient, a matrix interpolation model has been developed and validated [2, 3, 1]. This interpolation is appropriate to model Doppler broadening, coolant density or control rods effects for thermal spectrum PWR reactors as well as for the homogeneous Molten Salt Fast Reactor (MSFR). Regarding heterogeneous fast spectrum reactors, the sensitivity to the crossed cells has to be considered on the matrices calculations, due to the large migration area. This has required the development of a new interpolation model.

The present paper describes this new interpolation model based on the calculation of the matrix sensitivity to local feedback effects, using a correlated sampling technique. Previous work [4, 5] has shown the efficiency of the correlated sampling technique association to the fission matrices on simple cases. Other work [6] illustrated the capability to calculate local density perturbation effect on fission matrices on homogeneous system with one group isotropic Monte Carlo. The model presented here has been developed to extend the TFM approach to the Sodium Fast Reactor (SFR) specificities. This technique consists in a modification of the neutron weight in order to be representative of a perturbed version of the reactor with a single Monte Carlo calculation. The new TFM interpolation model approach, detailed in section II., is based on the use of these perturbed weights to generate the matrices together with their perturbed version. The application of this interpolation model is presented in section III. together with direct Monte Carlo comparisons. The results obtained on the modelling of fuel temperature (Doppler broadening) and coolant (sodium density) perturbations are then detailed. The validity domain of the interpolation for important perturbations such as coolant boiling is also investigated in this paper, comparing the neutron source redistribution and the reactivity variation of the interpolation with direct Monte Carlo calculations. Finally, the interpolation model is also used in section IV. to estimate the distribution of point kinetic feedback coefficients for sodium and temperature perturbations, and also for a clad density perturbation corresponding to a relocalization during accidental situations. These results are presented, together with a comparison to ERANOS [7] calculations and a spectral analysis explaining the results obtained.

II. TFM APPROACH AND CORRELATED SAMPLING

1. Fission Matrices

The fission matrices are the numerical transposition of Green functions aiming to characterise the neutron propagation in the core. The Green function approach consists

in reconstructing the neutron propagation as a sum of local contributions, each contribution being the generation system response ($\nu\Sigma_f\psi$) to a Dirac-"source neutron emission". Due to the Monte Carlo process, the estimation of these Green functions is based on an arbitrary volume discretization subscripted on i, j, k. For each possible neutron emitted in j, its fission neutron production $\nu\Sigma_f\psi$ is estimated in each volume i. This production corresponds to the line i - column j term of the fission matrix $\underline{\underline{G}}$ that condenses the whole transport neutron information during one generation. The objective of the perturbative approach discussed here is to include the sensitivity to a perturbation localized in volume k on this production.

Note that different kinds of matrices are estimated for the TFM approach. The neutron behavior is different depending on its emission spectrum (prompt or delayed), and the neutron prompt and delayed productions have to be considered distinctly. For this reason, the four matrices $\underline{\underline{G_{\chi_p\nu_p}}}$, $\underline{\underline{G_{\chi_p\nu_d}}}$, $\underline{\underline{G_{\chi_d\nu_p}}}$, $\underline{\underline{G_{\chi_d\nu_d}}}$ are estimated during the same Monte Carlo calculation, tagging the neutron type for the neutron spectrum and scoring both neutron multiplicities $\nu_p\Sigma_f\psi$ and $\nu_d\Sigma_f\psi$. Note that the neutron spectrum refers to the emission position j and the neutron multiplicity refers to the neutron production position i. Finally the neutron propagation time is also stored in the time propagation matrix. These five matrices are used by the TFM approach to perform neutron kinetics, the fission matrices providing the generational variation of the prompt and delayed neutron distributions, and the time matrix providing the temporal information associated to the generations.

2. Correlated Sampling Technique

The estimation of a small difference between two different Monte Carlo calculations is suffered from statistical error since the statistical errors are independent. For example for the reactivity, a small perturbation on the sodium density that has an impact of one pcm would require two calculations with a statistical error much smaller than one pcm which is not realistic.

The correlated sampling technique is being used here to improve the estimation of the impact of a perturbation on the neutron path. As mentioned, it consists in associating a perturbed weight to each neutron in order to be representative of a perturbed version of the reactor. This weight is modified at each interaction to take into account that each event doesn't have the same probability to occur in the reference reactor and in a perturbed one. In this way, the different scores can be estimated using a single Monte Carlo calculation for both the reference and the perturbed system with the same neutron histories. Finally, these two estimations have the same statistical error, thus their difference provides a much more precise evaluation of the perturbation on the reactivity or any other scored quantity. Note that if the considered material is not locally perturbed or if the region is voided, the neutron perturbed weight is not modified.

Two kinds of weight perturbation are considered. Considering a given reaction r on the nucleus n at the distance d, with a cross section $\Sigma_{n,r}$ and a total cross section Σ_{tot}, the probability to sample this distance is $\Sigma_{tot}\exp(-d\cdot\Sigma_{tot})$ and to sample this reaction is $\Sigma_{n,r}/\Sigma_{tot}$. The neutron weight modification due to a perturbation is the ratio of the perturbed probability and the reference one. Considering the distance sampling, the neutron perturbed weight is multiplied by:

$$\frac{\Sigma_{tot}^{pert}\exp(-d\cdot\Sigma_{tot}^{pert})}{\Sigma_{tot}\exp(-d\cdot\Sigma_{tot})} \quad (1)$$

Considering the reaction type sampling, the neutron perturbed weight is multiplied by:

$$\frac{\Sigma_{n,r}^{pert}\cdot\Sigma_{tot}}{\Sigma_{tot}^{pert}\cdot\Sigma_{n,r}} \quad (2)$$

This is a multiplicative process, the neutron weight being modified after each interaction. Each fission has a perturbed weight that results from the multiplication of all the weight modifications of the neutron during its propagation. This perturbed weight is transmitted to the new neutrons produced by the fission, and then to all the future neutron generations, in order to take into account the perturbation of the neutron source. To avoid the accumulation over generations of a large difference between the perturbed weights of the simulated neutrons, this transmission of perturbed weights is limited to a maximum number of generations depending on the reactor.

3. Correlated Sampling Application to the Fission Matrices

The fission matrices require the estimation of all the i,j elements that correspond to a $\nu\Sigma_f\psi$ score discretized on the fission position i and neutron creation j volumes. This $\nu\Sigma_f\psi$ quantity is multiplied by the perturbed neutron weight to generate the matrices of the perturbed reactor.

In order to model the effect of various local perturbations on the fission matrices with the same Monte Carlo calculation, different perturbed weights are associated to each neutron. The perturbed weights are discretized according to each volume k, each associated weight corresponding to a given local perturbation in k. Finally, with two different perturbations (e.g. coolant density and media temperature), the number of perturbed weights associated to each neutron is $2\cdot k$.

All the fission and time matrices are generated for each perturbed weight in k. For the matrix $\underline{\underline{G_{\chi_p\nu_p}}}$, we write $\underline{\underline{\widetilde{G}^{\text{den k}}_{\chi_p\nu_p}}}$ and $\underline{\underline{\widetilde{G}^{\text{dop k}}_{\chi_p\nu_p}}}$ the "*variation matrices*" generated with the correlated sampling technique, corresponding to the variation of $\underline{\underline{G_{\chi_p\nu_p}}}$ due to a local perturbation of the coolant density and of the temperature in k.

The neutron weight propagation through generations, required for the correlated sampling technique, has been implemented and can be used for the calculation of $\underline{\underline{\widetilde{G}^{\text{den k}}_{\chi_p\nu_p}}}$ and $\underline{\underline{\widetilde{G}^{\text{dop k}}_{\chi_p\nu_p}}}$. However, thanks to the capability of the fission matrices to predict the perturbed neutron source through the Eigen vector, this propagation of the neutron weight is not required if the mesh discretization is fine enough and the generated matrices are identical with and without neutron weight propagation. For a given configuration, a sensitivity study on the mesh discretization is required.

4. Interpolation of the Fission Matrices

In order to estimate the modification of the fission matrices due to an arbitrary perturbation amplitude and distribution, the variation matrices can be used to interpolate the fission matrices. The global perturbation is reconstructed as a sum of local perturbations, together with a linear interpolation for the density effect and a logarithmic interpolation for the Doppler effect. For any matrix $\underline{\underline{G_{\chi_x\nu_x}}}$ of the TFM approach, the interpolated matrix with a density and a temperature perturbations is calculated using Eq. (6).

$$\begin{aligned}\underline{\underline{G_{\chi_x\nu_x}}}(\Delta\rho_{\text{sodium}}(\text{k}),\text{T}(\text{k})) = \ & \underline{\underline{G_{\chi_x\nu_x}}} \\ & + \sum_{\text{k}} \underline{\underline{\widetilde{G}^{\text{den k}}_{\chi_x\nu_x}}} \cdot \Delta\rho_{\text{sodium}}(\text{k}) \\ & + \sum_{\text{k}} \underline{\underline{\widetilde{G}^{\text{dop k}}_{\chi_x\nu_x}}} \frac{\log(T(\text{k})/T_{\text{ref}}(\text{k}))}{\log((T_{\text{ref}}(\text{k})+300)/T_{\text{ref}}(\text{k}))}\end{aligned} \tag{3}$$

5. Source Neutron Redistribution and Reactivity Estimation

The interpolated matrix is representative of the local neutron propagation in the perturbed system. Considering a time step t associated to a perturbation shape $(\Delta\rho_{\text{sodium}}(\text{k}),\text{T}(\text{k}))$, the Eigen vector $\boldsymbol{N}_{\text{p}}(t)$ of the matrix $\underline{\underline{G_{\chi_p\nu_p}}}(t) = \underline{\underline{G_{\chi_p\nu_p}}}(\Delta\rho_{\text{sodium}}(\text{k}),\text{T}(\text{k}))$ is solution of the Eq. (4) and corresponds to the equilibrium neutron distribution. The associated Eigen value is the prompt multiplication factor of the system.

$$\underline{\underline{G_{\chi_p\nu_p}}}(t)\boldsymbol{N}_{\text{p}}(t) = k_{\text{p}}(t)\boldsymbol{N}_{\text{p}}(t) \tag{4}$$

In order to take into account the coupled effects between prompt and delayed neutrons, we use the $\underline{\underline{G_{\text{all}}}}(t)$ block-matrix (Eq. 5) constructed with the "prompt to prompt" and "delayed to delayed" matrices on the diagonal, and the crossed productions out of the diagonal. The Eigen vector $\boldsymbol{N}_{\text{eq,all}}(t) = \left(\boldsymbol{N}_{\text{p,eq}}(t)\ \boldsymbol{N}_{\text{d,eq}}(t)\right)$ corresponds to the prompt and delayed distribution in the reactor at equilibrium, and the associated Eigen value is the effective multiplication factor $k_{\text{eff}}(t)$ of the reactor.

$$\underline{\underline{G_{\text{all}}}}(t) = \begin{pmatrix} \underline{\underline{G_{\chi_p\nu_p}}}(t) & \underline{\underline{G_{\chi_d\nu_p}}}(t) \\ \underline{\underline{G_{\chi_p\nu_d}}}(t) & \underline{\underline{G_{\chi_d\nu_d}}}(t) \end{pmatrix} \tag{5}$$

III. APPLICATION OF THE TFM APPROACH WITH THE PERTURBATIVE INTERPOLATION MODEL

1. Application Case Presentation

The development of this perturbative interpolation model has been performed in the general framework of the low void effect [8] sodium fast reactor ASTRID. This kind of concept is characterized by a large sodium plenum increasing the neutron leakage in case of a sodium density decrease.

A simplified geometry of a 1D assembly has been considered as application case to check the capability of this approach to be representative of the physics involved in this kind of reactor with the variation of the flux gradient in case of sodium loss. The geometry, composed of three areas (fissile, sodium and B_4C), is represented in Fig. 1 and the material temperatures and isotopic compositions are given in Table I. These compositions are considered radially homogeneous. The geometry boundary condition is a radial reflexion and axial leakage. Note that the fuel region here corresponds to an assembly homogenization so that it contains fuel, sodium and steel.

Fiss - 1500 K		Na - 600 K		B_4C - 600 K	
^{16}O	1.952e-02	^{23}Na	2.106e-02	^{10}B	6.388e-03
^{23}Na	6.352e-03			^{11}B	2.587e-02
^{56}Fe	1.861e-02			^{12}C	8.065e-03
^{235}U	1.542e-05			^{23}Na	1.094e-02
^{238}U	7.599e-03			^{56}Fe	1.256e-02
^{238}Pu	5.833e-05				
^{239}Pu	1.238e-03				
^{240}Pu	5.773e-04				
^{241}Pu	1.617e-04				
^{242}Pu	1.743e-04				
^{241}Am	2.713e-05				

TABLE I. Material temperatures and compositions - 10^{24} atoms per cm^3

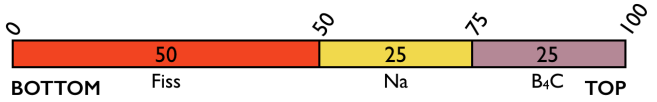


Fig. 1. Case geometry description in cm.

All the calculations presented in this paper have been performed with a modified version of the neutron Monte Carlo code Serpent [9] and with the JEFF3.1 database. One billion of neutrons have been simulated per calculation and a 60 bins geometry discretization for i j and k is considered. A sensitivity study has been performed: the results detailed in the article are identical using a finer 120 bins mesh, and also using a propagation of the neutron perturbed weight on 8 generations. The source neutron distribution in the system is presented in Fig. 2 (left). We can notice the asymmetry of this distribution in the fuel due to the large neutron leakage at the bottom of the geometry (left part of the figure). The neutron reflection contribution of the sodium plenum is directly visible with the large amount of neutrons created in the fuel near to the sodium: without the reflection of the sodium, the neutron source at 50 cm would be equivalent to the one at 0 cm. For this reason, the leakages are increased accordingly if the sodium density is reduced.

The neutron production shape corresponds to the Eigen vector of the fission matrix $\underline{\underline{G_{\chi_p\nu_p}}}$ displayed in Fig. 2 (right). Each column j of the fission matrix corresponds to the propagation of the neutron in the i volumes. Considering an emission in the center of the fuel (ie. column $j = 15$ of the matrix), each line of this column represents the probability that a neutron produces a fission neutron during one generation. This proba-

bility is zero in the sodium (bins 30-44) and in the B_4C areas (bins 45-59). The values on the diagonal (j = i) correspond to the neutron production at the same place as the neutron emission, which is the most probable fission position. The general diagonal shape of this matrix shows the propagation of the fissions around the neutron emission, the values far from the diagonal correspond to large migration areas.

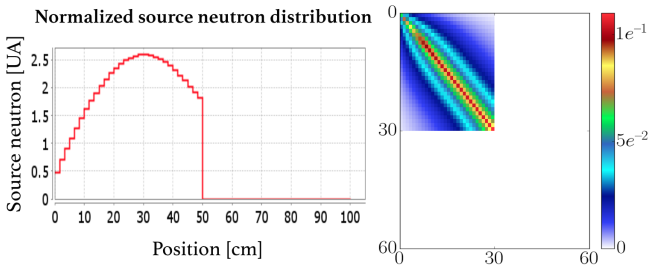


Fig. 2. Source neutron distribution (left) and reference $\underline{\underline{G_{\chi_p \nu_p}}}$ matrix (right).

2. Matrix Calculations

Using the correlated sampling technique, different variation matrices are generated. The matrices presented in Fig. 3 are the variation of the $\underline{\underline{G_{\chi_p \nu_p}}}$ matrix due to a local perturbation in k of the sodium density or of the fuel temperature. We consider in this paper a reference estimation of these matrices for a sodium density perturbation of -1% and for a temperature perturbation of +300K.

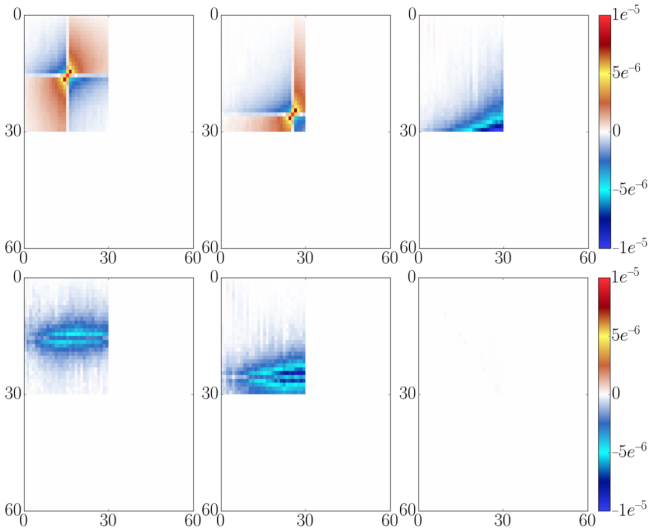


Fig. 3. Variation matrices $\underline{\underline{\widetilde{G}^{\text{den k}}_{\chi_x \nu_x}}}$ (top) and $\underline{\underline{\widetilde{G}^{\text{dop k}}_{\chi_x \nu_x}}}$ (bottom) for a perturbation in volumes 15 (left), 25 (middle) and 40 (right).

A local variation of the sodium density of -1% produces a redistribution of the neutron propagation with a strong discontinuity around the perturbation position k. If the emission and the fission position are on the same side, (i and j) > k or (i and j)< k, the impact of the perturbation is a decrease of the fission neutron production. At the opposite, if the perturbation is located between i and j, the neutron production is increased because the spectrum becomes harder. The effect of a sodium density decrease in the sodium plenum is a strong fission production reduction near to the sodium area due to the neutron leakage in the B_4C.

Concerning the Doppler effect, it produces a global decrease of the fission production around position k. The Doppler broadening favours the absorptions, and this effect is more important for a perturbation near to the sodium area where the spectrum is softer.

3. Interpolation of the Matrices and Validation

In order to validate the interpolation model and the implementation of the approach, two configurations have been considered. A perturbation of the reactor with a different shape and amplitude has been calculated with a variation of the sodium density of -2% in the sodium area, and a variation of -300K at the top of fuel area. In this way this checks the interpolation based on the reference variation of the sodium density of -1% and of the temperature of +300K (reference matrices). The interpolated fission matrices corresponding to these perturbations are calculated using:

$$\begin{aligned} \underline{\underline{G_{\chi_x \nu_x}}}^{-2\%\text{Na}} &= \underline{\underline{G_{\chi_x \nu_x}}} + \sum_{\text{k}\in\{30,44\}} \underline{\underline{\widetilde{G}^{\text{den k}}_{\chi_x \nu_x}}} \cdot 2 \\ \underline{\underline{G_{\chi_x \nu_x}}}^{-300\text{K}} &= \underline{\underline{G_{\chi_x \nu_x}}} + \sum_{\text{k}\in\{15,29\}} \underline{\underline{\widetilde{G}^{\text{dop k}}_{\chi_x \nu_x}}} \frac{\log(1200/1500)}{\log(1800/1500)} \end{aligned} \tag{6}$$

We remind here that the reference matrices are calculated using direct Monte Carlo calculations, without using the correlated sampling technique. Two distinct Monte Carlo calculations are performed, for the perturbed and the reference system, and the difference of the generated fission matrices provides the reference values for $\underline{\underline{G_{\chi_x \nu_x}}}^{-2\%\text{Na}}$ and $\underline{\underline{G_{\chi_x \nu_x}}}^{-300\text{K}}$.

The results obtained are presented in Fig. 4. The results of the interpolation model are represented on the left, the reference estimation using direct Monte Carlo calculation are represented in the middle, and the difference between these two estimations are represented on the right. For both density and Doppler effects, the global shapes are very well reproduced by the interpolated matrices and the differences are due to the statistical errors only.

In addition to the fission matrix comparison, a second point is the validation of the redistribution shape prediction. For this, the Eigen vector of the interpolated matrix is compared to the estimation of the source neutron shape difference of the two Monte Carlo direct calculations. The two configurations are represented in Fig. 5. For the density perturbation (red) and the Doppler perturbation (blue), the interpolated results (dashed line) perfectly reproduce the Monte Carlo calculation (solid line).

Finally, the Eigen values associated to the interpolated matrices are compared to the reactivity variations of the Monte Carlo direct estimation in table II. Once again the interpolation model shows its capability to precisely predict the reactivity variation due to a perturbation in the system.

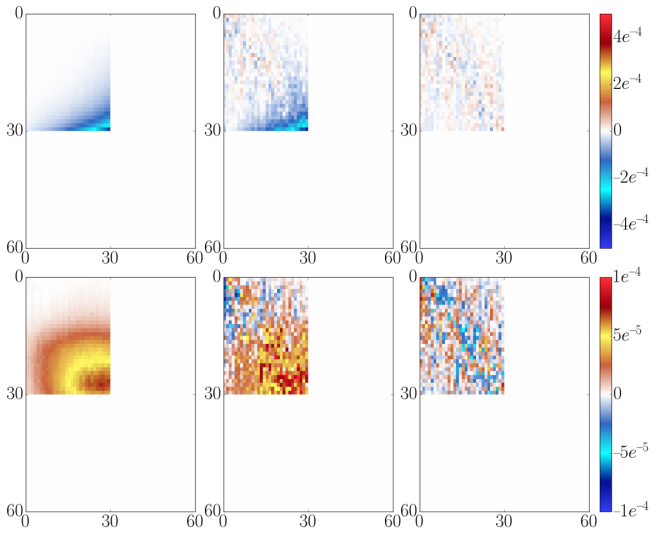


Fig. 4. Fission matrix variation due to a local variation of the sodium density of −2% in the sodium plenum (top) and to a local variation of the temperature of −300K (bottom): results of the interpolation model (left), direct Monte Carlo calculation (middle) and difference (right).

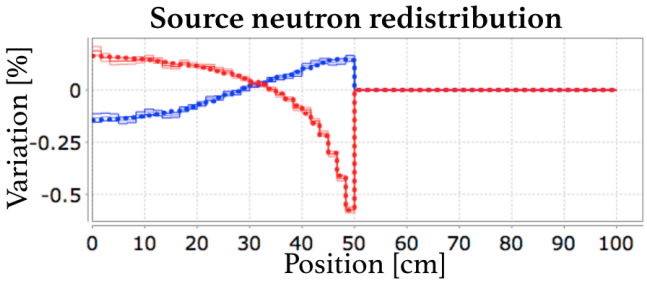


Fig. 5. Source neutron redistribution due to a local variation of the sodium density (red) and of the temperature (blue): results of the interpolation model (dashed line) and of the direct Monte Carlo calculation together with the statistical error (solid line).

4. Interpolation of the Matrices for Large Perturbations

The fission matrice interpolation uses variation matrices $\widetilde{\overline{\overline{G}}}_{\chi_x \nu_x}$ calculated with a small perturbation around the nominal state. Using these matrices may induce a bias if we consider large perturbations of the reactor compared to the nominal state due to a potential non-linear behavior. Note that this interpolation model does not assume that the flux redistribution is linear at the system scale, but that the *local* system response on one generation is linear. In this section, large sodium variations are considered as illustration since this phenomenon produces the larger flux redistribution in the core.

Two characteristic amplitudes are considered: a variation of -15 % that is the order of magnitude of the sodium density variation before sodium boiling, and a variation of -100 % that corresponds to a total void effect. Four perturbation localizations have been calculated in order to obtain distinct characteristic behaviors: case A in the bottom of the fissile region (0 cm up to 25 cm), case B in the upper part of the fissile region (25 up to 50 cm), case C in the first 10 cm of the sodium region (50 cm up to 60 cm), and case BC that combines B and C (25 cm up to 60 cm). Each case represented in Fig. 6 is declined for the two amplitudes mentionned.

Case	density$^{50-75\ cm}$	Doppler$^{25-50\ cm}$
$\Delta\rho_{ref}$	-60 ± 3	69 ± 3
$\Delta\rho_{interpolation}$	-60.7	67.8
difference	(1 ± 5) %	(-2 ± 5) %

TABLE II. Reactivity variation due to a local variation of the sodium density and of the temperature

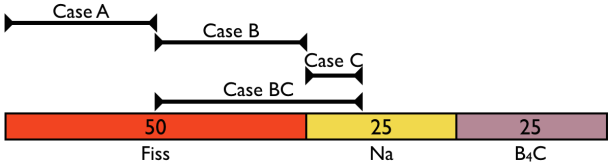


Fig. 6. Position of the perturbation in cases A,B,C and BC.

The results obtained with the sodium density perturbation at -15 % and -100 % are respectively presented in Figs 7 and 8, and the reactivity in Tables III and IV. As previously illustrated, the non-zero terms of the matrices are only in the 0-30 bins (corresponding to the fissile area in 0-50 cm). For each case, the reference calculation (middle) corresponds to two direct Monte Carlo calculation with the corresponding sodium modification shape and amplitude: the variation matrix is the difference between the perturbed and the reference matrices. Note the two distinct Monte Carlo used for this reference calculation are performed with one billion of neutron, while all the matrices required for the interpolation (left) are calculated using only one calculation with also one billion of neutrons.

Different observations can be done concerning the physics of the matrices variation independently of the perturbation amplitude (Figs. 7 and 8):

- Concerning case B, a decrease of the fission probability along the diagonal is observed in the upper fissile area. This effect is due to the increase of the neutron mean free path. An important increase of the fission probability is observed far from the diagonal due to the sodium density decrease that implies a harder neutron spectrum.
- If the sodium perturbation is near to the bottom of the fissile area (case A), the effect on the matrix is almost the same but the proximity of the bottom boundary reduces the fission probability far from the diagonal.
- For a perturbation in the sodium area (case C), the effect is a depletion of the fission matrix near to the sodium.
- For a perturbation combining cases B and C, the resulting matrix is the sum of the two corresponding matrices.

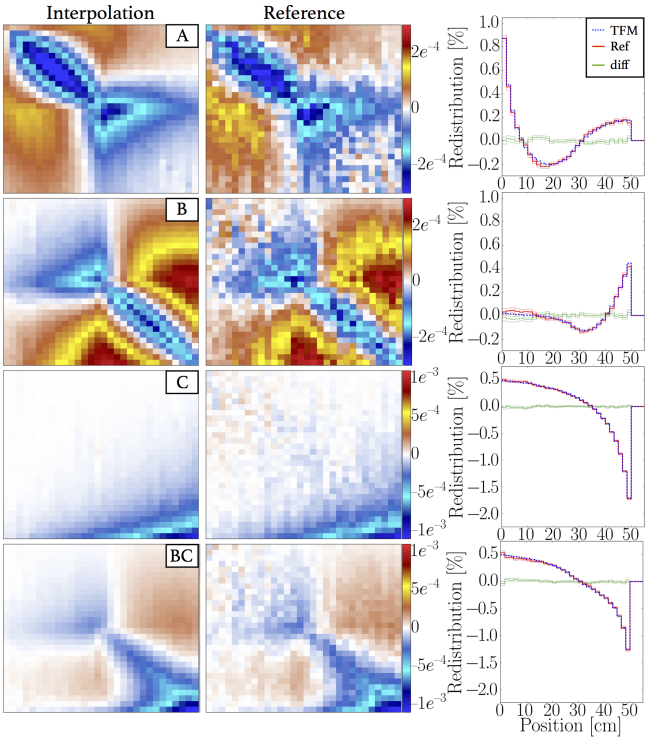


Fig. 7. TFM interpolated matrix variation (bins 0-30) associated to the -15 % sodium variation (left), reference matrix variation (middle) and comparison of the associated source neutron redistributions.

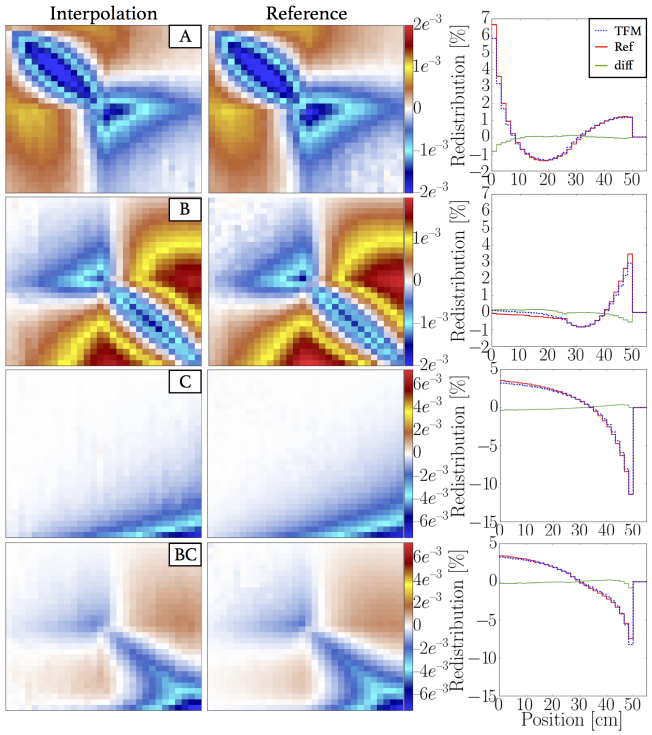


Fig. 8. TFM interpolated matrix variation (bins 0-30) associated to the -100 % sodium variation (left), reference matrix variation (middle) and comparison of the associated source neutron redistributions.

Case	$\Delta\rho_{\text{ref}}$	$\Delta\rho_{\text{interpolation}}$	difference
A	-91 ± 2	-95	4 ± 2 %
B	92 ± 2	88	-4 ± 2 %
C	-181 ± 2	-183	1 ± 1 %
BC	-94 ± 2	-96	2 ± 2 %

TABLE III. Reactivity variation due to -15 % sodium variation from TFM and the Monte Carlo reference calculation

Case	$\Delta\rho_{\text{ref}}$	$\Delta\rho_{\text{interpolation}}$	difference
A	-747 ± 2	-637	-15 ± 0.2 %
B	686 ± 2	586	-15 ± 0.2 %
C	-1336 ± 2	-1212	-9 ± 0.1 %
BC	-762 ± 2	-638	16 ± 0.2 %

TABLE IV. Reactivity variation due to -100 % sodium variation from TFM and the Monte Carlo reference calculation

A perturbation in the sodium area implies an important decrease of the neutron source redistribution near to the upper fissile area (Fig. 7 - right, case C) due to the large increase of the neutron leakages in the B_4C. For a perturbation in the fuel, two opposite effects occur: the local mean free path increase tends to locally decrease the neutron redistribution, while a harder neutron spectrum tends to increase the fission rate. For this reason, we can see on cases A and B that the redistribution is almost negative in the perturbation position, and positive at the boundaries of the perturbation with a large influence of the material next to the perturbation (sodium, unperturbed fuel or leakage).

With the -15 % sodium density variation, the amplitude of the variation matrices is limited compared to the -100 %, and thus the reference and the perturbed fission matrices estimated using two distinct Monte Carlo calculations are not significantly different. Since the statistical errors are independent, the reference variation matrix that is the difference between the two calculated matrices has a large statistical error. This effect is reduced for the -100 % since the residual statistical error is much smaller than the difference of the perturbed and reference matrices. A good global agreement is obtained in both cases, the behavior of the neutron local propagation is correctly reproduced. Note that the feedback is positive for case B since the harder spectrum tends to increase the reactivity, while it is negative for case A due to the increased neutron leakages. This effect will be discussed in section IV. with the point kinetic feedback coefficients estimation.

The neutron source redistributions (right column) are also correctly reproduced. The agreement is very good for a -15 % perturbation, and a small difference appears for the total void configuration.

The reactivity variations are also reproduced with a very good agreement for the -15 % perturbation (Table III), the

maximum difference being of 4% on the reactivity variation. The limit of the interpolation appears with a -100 % perturbation (Table IV). For a total void effect, the reactivity variation is predicted with a maximum bias of 16 %. Even if the global shape of the matrices is good and then their Eigen vectors (source neutron distributions) are correct, the Eigen values (multiplication factors) are very sensitive to the non-linearity for a local total void configuration. A possible solution that can be investigated for future developments is to estimate the variation matrices at different intermediate densities between 100% and 0%, and finally to interpol the final matrix with these intermediate matrices.

IV. POINT KINETIC LOCAL FEEDBACK DISTRIBUTION

1. Feedback Calculations

The objective of the initial development of the TFM approach was the calculation of effective kinetic parameters and the capability to perform spatial kinetic calculations. From the new developments presented here, local feedback coefficients can also be calculated by using the variation matrices. The TFM approach can thus provide Monte Carlo based point kinetics precise parameters to other calculation codes.

Each variation matrix corresponds to a local perturbation in the reactor (material density and Doppler broadening in this work). The effective multiplication factor associated to this perturbation is directly given by the Eigen value of $\underline{\underline{G_{\text{all}}}} + \underline{\underline{\widetilde{G}^{\text{k}}_{\text{all}}}}$. Finally the reactivity variation associated to each local perturbation in the volumes k is calculated using TFM.

Note that the corresponding Eigen vector can also be calculated for each k value. Assuming that the impact of the variation of the neutron source distribution due to a system modification in cell k is negligible on the propagation of another modification in cell k′ in the reactor, then a pseudo spatial kinetic model can be established. This model uses at each time step a sum of variation vectors weighted by the amplitude of the system modification in k. In this way the calculation time would be very fast, but this approach can not be able to observe neutron decoupling effect.

In order to have a comparison for the feedback coefficients obtained, S_N calculations with 33 energy groups have been performed with the ERANOS code [7]. These deterministic calculations are based on the traditional two level lattice/core scheme and the JEFF 3.1 nuclear database. First, self-shielded cross sections are computed by the ECCO code cell, using the fundamental mode assumption for all the materials of the 1D core geometry. For fissile materials, a buckling search algorithm is used to obtain the critical flux for the cross section collapsing to a 33 energy group mesh. For the subcritical materials such as fertile or structural parts of the 1D sub-assembly, the process is based on source calculations using the spectrum coming from previous fissile calculations. The boundary conditions are a flux leakage on the axial boundaries for both cases, and no volumetric leakage are considered since there is no radial leakage for this application case.

Figure 9 shows the density (left) and Doppler (right) feedbacks coefficient calculated for the system. The density feedbacks are calculated for a sodium and clad density variation of -1 %. This Doppler feedback is calculated with a logarithmic dependency due to the temperature perturbation amplitude in the correlated sampling process (+300 K). A very good agreement is obtained between TFM (red) and ERANOS (blue).

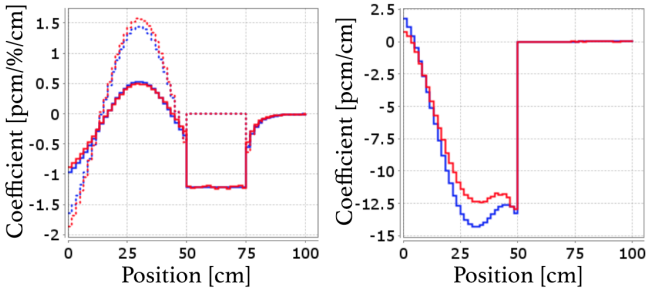


Fig. 9. Density feedback coefficient (left) associated to a local perturbation of -1 % in the sodium (plain line) and the steel (dashed line), and Doppler logarithmic coefficient (right) calculated as $\frac{\Delta\rho}{\log(T+300/T)}$, with TFM (red) and ERANOS (blue).

Concerning the density effect, the feedbacks are different in the three regions. In the fuel region the sodium (plain line) and the steel (dashed line) feedbacks have the same behavior, the amplitude being larger for the steel due to the larger absorptions in this media. Near to the fuel boundaries, the feedback is negative since a decrease of the nuclei density increases the local neutron mean free path, and then the leakages. In the middle of the fuel region the feedbacks are positive, indeed the decrease of the sodium density makes the neutron spectrum harder, together with the absorption decrease in the steel if its density is reduced.

In the B_4C, the feedbacks are negative since the presence of sodium and steel reduces the absorptions on the boron due to the reflections. In the sodium plenum, the only component is sodium without any steel and the clad feedback is thus null here. We can see that the sodium feedback value is constant in this region. The impact on the reactivity is exactly the same if the perturbation is near to the fissile (eg. at 55 cm) or near to the B_4C (eg. 70 cm) even if the neutron flux and importance are reduced in the latter. Such an effect was expected with this one dimensional geometry without radial leakages. The only leakages are axial, and for the reason, the probability that a neutron leaving the fissile area arrives in the B_4C only depends on the total amount of sodium nuclei between these two regions. The reflector capability of the sodium in this region only depends on the total amount of sodium and not of its distribution.

Concerning the Doppler effect, this effect is mainly negative since the Doppler broadening favors the absorption/fission ratio. Between 0 cm and 5 cm the Doppler effect is positive: the total cross section increase limits the leakage on this part

of the geometry. An important local variation may be observed near to the fissile-sodium interface. Indeed the reflected neutrons returning from the sodium area have a softer spectrum which directly impacts the Doppler broadening sensitive to the neutron spectrum.

A slight difference is obtained between TFM (red) and ERANOS (blue). This difference is due to the important spectral variation detailed in the next section. The neutron spectrum variation is also large between the sodium and the fissile areas, meaning that the fundamental mode assumption may no be appropriate. Finally, another possible origin for this discrepancy is the self-shielded multigroup cross section anisotropy. A neutron reflected from the sodium down to the fuel area comes back with a smoother spectrum, and due to the progressive spectrum variation inside the fissile, the self-shielded cross sections may be different depending on the neutron direction.

2. Spectral analysis

In order to confirm the origin of the difference between deterministic and TFM based Doppler feedback coefficients, spectrum maps have been generated and are detailed here. These maps, evaluated with the Serpent Monte Carlo code, consist in a flux score in the system with a double discretization: axially (500 bins in ordinate) and in lethargy (5000 bins in abscissa). The Serpent code has been modified to obtain an additional information for each neutron: the direction of its axial velocity, positive if the neutron goes from the bottom to the top of the assembly, and negative elsewhere.

The first maps (Fig. 10) represent the flux repartition in the system. The A map corresponds to the direct flux for each lethargy-position bin, while the B and C maps represent the map flux of the neutrons with respectively a positive and negative axial velocity. The D map represents the relative difference between B and C.

We can see that the mean neutron energy in the fissile region (between 0 and 50 cm) is equal to around 300 keV even if the neutrons are produced here at around 2 MeV, due to scattering in the fuel. Then the neutrons that move to the sodium area are thermalized as observed between 50 and 70 cm. The fast component (1-10 MeV) is cut within a few centimeters in the sodium. The component around 100 keV is more important and we can see the accumulation of a neutron population around 1keV, below the sodium absorption resonance that depletes the neutron spectrum map. We can note the large number of resonances in the fissile area compared to the sodium area, especially at low energy.

As explained, map D represents the difference between the up and down velocity components. Using the S_N transport solver for the ERANOS code, the strong flux anisotropy that is directly visible on this D map is correctly taken into account.

We need to go further to understand the difference between ERANOS and TFM. Figure 11 represents the spectrum maps: it corresponds to the flux map but normalized in each position bin in order to see how the neutron spectra are modified inside the geometry.

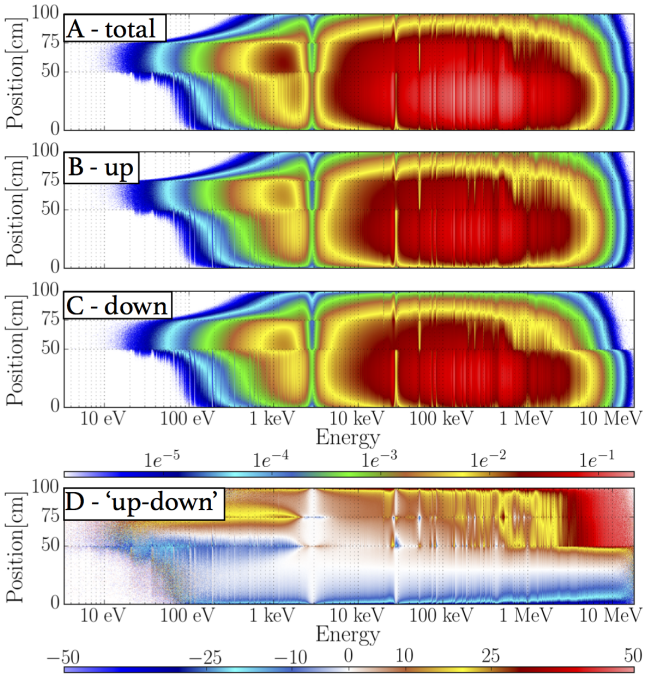


Fig. 10. Neutron flux normalized per source neutron: the "A" map represents the total flux, the "B" and "C" maps represent the neutrons with respectively a positive (up) and a negative (down) axial velocity, and the difference of "B-C" is presented in map "D" in percents of the average values.

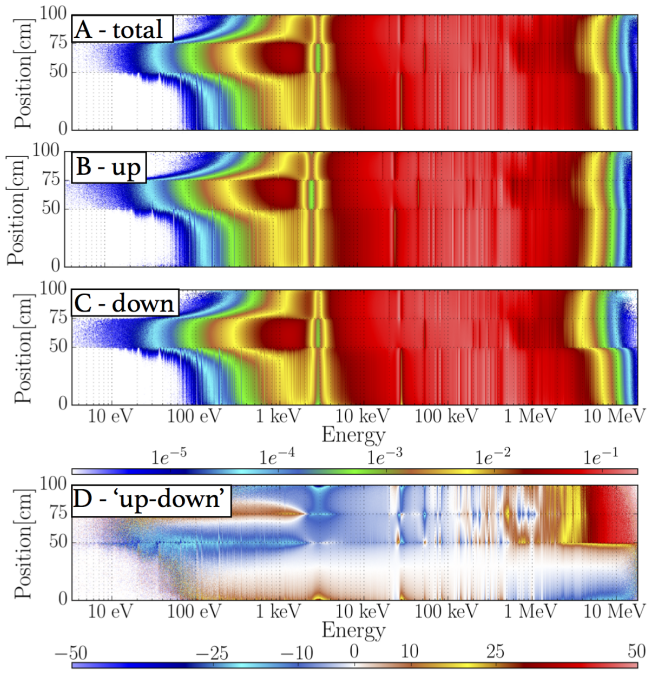


Fig. 11. Neutron spectra normalized per axial bin: the "A" map represents the total spectra, the "B" and "C" maps represent the neutrons with respectively a positive (up) and a negative (down) axial velocity, and the difference of "B-C" is presented in map "D" in percents of the average values.

We can see on map D that the neutron spectrum needs a few tens centimeters to be converged on a "fundamental spectrum" between each material interface. Additionally, we can see a strong spectral anisotropy in the energy range of the resonances. For these reasons, the fundamental mode assumption may be not appropriate on this kind of geometry where the fuel height is small, and new calculation schemes considering anisotropy and axial dependence in the self-shielded cross sections should provide better results.

V. CONCLUSIONS

The present work provides an innovative way to predict the neutron redistribution and the reactivity variation due to a perturbation in a fast spectrum heterogeneous reactor. The paper demonstrates the capability to interpolate fission matrices on the fly for a given shape and amplitude of coolant density and material temperature using a sum of local contribution. Thanks to a correlated sampling technique, the effect of different local perturbations on the fission matrices are estimated using a single Monte Carlo calculation and with a small statistical error. The precision obtained with this model on the neutron redistribution and on the reactivity is around the percent on a partial assembly representative of the low void effect of the ASTRID reactor.

Perturbations with large amplitude have also been tested to investigate the limits of this interpolation model. A sodium variation up to -15 % that corresponds to the limit before boiling is reproduced with a very good agreement compared to direct Monte Carlo calculations. A variation of -100 % that corresponds to a local total void effect is predicted with a good agreement on the neutron redistribution but a bias of 16 % on the reactivity variation due to the non-linearities.

Finally point kinetics feedback distributions have been sucessfully calculated with this Monte Carlo based approach, and compared to the ERANOS deterministic code.

This model can be used for future applications to perform precise neutron kinetics with a coupling to the thermal-hydraulics, only one Monte Carlo calculation being required prior to the transient and all the interpolations being performed with a reduced computation time.

VI. ACKNOWLEDGMENTS

The authors wish to thank the CEA (Commissariat à l'Energie Atomique et aux Energies Alternatives) and the IN2P3 department of the CNRS (National Center of for Scientific Research) for their support.

REFERENCES

1. A. LAUREAU, M. AUFIERO, P. RUBIOLO, E. MERLE-LUCOTTE, and D. HEUER, "Transient Fission Matrix: Kinetic calculation and kinetic parameters β_{eff} and Λ_{eff} calculation," *Annals of Nuclear Energy*, **85**, 1035–1044 (2015).
2. A. LAUREAU, *Développement de modèles neutroniques pour le couplage thermohydraulique du MSFR et le calcul de paramètres cinétiques effectifs*, Ph.D. thesis, Université Grenoble Alpes (2015).
3. A. LAUREAU, M. AUFIERO, P. RUBIOLO, E. MERLE-LUCOTTE, and D. HEUER, "Coupled neutronics and thermal-hydraulics transient calculations based on a fission matrix approach: application to the Molten Salt Fast Reactor," in "Joint International Conference on Mathematics and Computation, Supercomputing in Nuclear Applications and the Monte Carlo Method (M&C+ SNA+ MC 2015), Nashville, USA," .
4. W. MATTHES, "Calculation of reactivity perturbations with the Monte Carlo method," *Nuclear Science and Engineering*, **47**, *2*, 234–237 (1972).
5. V. BERNNAT, "A MONTE CARLO TECHNIQUE FOR LOCAL PERTURBATIONS IN MULTIPLYING SYSTEMS," (1974).
6. A. MAJUMDAR and W. R. MARTIN, "Multiple reactivity calculation using single correlated sampling Monte Carlo simulation," in "Proceedings of Reactor Physics," pp. 85–93 (1994).
7. G. RIMPAULT, D. PLISSON, J. TOMMASI, R. JACQMIN, J. RIEUNIER, D. VERRIER, and D. BIRON, "The ERANOS code and data system for fast reactor neutronic analyses," in "Proc. Int. Conf. PHYSOR," (2002), vol. 2, pp. 7–10.
8. P. SCIORA, D. BLANCHET, L. BUIRON, B. FONTAINE, M. VANIER, F. VARAINE, C. VENARD, S. MASSARA, A.-C. SCHOLER, and D. VERRIER, "Low void effect core design applied on 2400 MWth SFR reactor," in "International Congress on Advances in Nuclear Power Plants (ICAPP)," (2011).
9. J. LEPPÄNEN, M. PUSA, T. VIITANEN, V. VALTAVIRTA, and T. KALTIAISENAHO, "The Serpent Monte Carlo code: Status, development and applications in 2013," *Annals of Nuclear Energy*, **82**, 142–150 (2015).